Molecular Phylogenetics and Evolution 67 (2013) 28–37

Contents lists available at SciVerse ScienceDirect

Molecular Phylogenetics and Evolution

journal homepage: www.elsevier.com/locate/ympev

Molecular phylogenetic evidence for the reorganization of the Hyperiid amphipods, a diverse group of pelagic crustaceans

Carla Hurt [a], Steven H.D. Haddock [b], William E. Browne [a,*]

[a] University of Miami, Cox Science Center, 1301 Memorial Drive, Miami, FL, 33146, United States
[b] Monterey Bay Aquarium Research Institute, 7700 Sandholdt Road, Moss Landing, CA, 95039, United States

ARTICLE INFO

Article history:
Received 22 May 2012
Revised 20 December 2012
Accepted 28 December 2012
Available online 11 January 2013

Keywords:
Amphipoda
Hyperiidea
Oceanic midwater environment
Molecular phylogeny
Species tree
Evolution

ABSTRACT

Within the crustaceans, the Amphipoda rank as one of the most speciose extant orders. Amphipods have successfully invaded and become major constituents of a variety of ecosystems. The hyperiid amphipods are classically defined as an exclusively pelagic group broadly inhabiting oceanic midwater environments and often having close associations with gelatinous zooplankton. As with other amphipod groups they have largely been classified based on appendage structures, however evidence suggests that at least some of these characters are the product of convergent evolution. Here we present the first multi-locus molecular phylogenetic assessment of relationships among the hyperiid amphipods. We sampled 51 species belonging to 16 of the 23 recognized hyperiidian families for three nuclear loci (18S, 28S, and H3) and mitochondrial COI. We performed both Bayesian Inference and Maximum Likelihood analyses of concatenated sequences. In addition, we also explored the utility of species-tree methods for reconstructing deep evolutionary histories using the Minimize Deep Coalescence (MDC) approach. Our results are compared with previous molecular analyses and traditional systematic groupings. We discuss these results within the context of adaptations correlated with the pelagic life history of hyperiid amphipods. Within the infraorder Physocephalata (Bowman and Gruner, 1973) we inferred support for three reciprocally monophyletic clades; the Platysceloidea, Vibilioidea, and Phronimoidea. Our results also place the enigmatic Cystisomatidae and Paraphronimidae at the base of the infraorder Physosomata (Bowman and Gruner, 1973) suggesting that Physosomata as traditionally recognized is paraphyletic. Based on our multilocus phylogeny, major rearrangements to existing taxonomic groupings of hyperiid amphipods are warranted.

1. Introduction

The Hyperiidea are an exclusively pelagic group of amphipod crustaceans (Martin and Davis, 2001). The hyperiids are a major constituent of crustacean zooplankton (Bowman and Gruner, 1973) and in some regions their swarming behavior can account for the primary food source of large planktovores (Vinogradov et al., 1996) as well as one of the major sources of mortality for gelatinous organisms (Mills, 1993). Despite their clear ecological importance, robustly supported molecular phylogenetic relationships within the Hyperiidea are nonexistent. In fact relationships among the higher level taxonomic groupings within the entire order Amphipoda remain unresolved, in large part due to conflicting suites of morphological characters currently used by systematists (Martin and Davis, 2001; Havermans et al., 2010; Hartke et al., 2011). These characters often include relatively subtle variations in bristle, spine, and setal patterns associated with appendages. The structure and anatomical position of these fine-scale cuticular features are developmentally labile characters and can show significant variation within species. Overall, morphology based reconstructions among and within the four major groups of Amphipoda suggests that convergent evolution may be playing a central role in amphipod evolution.

The Amphipoda are generally organized into the largely benthic taxa, the Gammaridea, Caprellidea, Ingolfiellidea, and the pelagic midwater taxon Hyperiidea (e.g., Martin and Davis, 2001). In comparison to the benthic, nearshore, and intertidal amphipods, hyperiids exhibit morphological traits correlated with their pelagic life history and commensal/parasitic associations with other zooplankton groups (Gasca et al., 2007; Harbison et al., 1977; Madin and Harbison, 1977). Some of these adaptations include hypertrophied olfactory and visual systems, duplications of the eyes, and a wide array of antennal and appendage modifications. However there is no known single morphological synapomorphy that unites the suborder Hyperiidea. Further the failure of traditional morphological analyses to identify relationships between higher level taxonomic groupings within the hyperiids suggests that potentially

* Corresponding author. Tel.: +1 305 284 3319.
E-mail address: wbrowne@bio.miami.edu (W.E. Browne).

1055-7903/$ - see front matter © 2013 Elsevier Inc. All rights reserved.
http://dx.doi.org/10.1016/j.ympev.2012.12.021

homoplasious morphological features may be masking true phylogenetic relationships among extant hyperiid amphipods. As a consequence, the notion of hyperiid polyphyly has also been suggested by some of the major taxonomic works on the suborder (reviewed in Vinogradov et al., 1996).

Where comparative morphological and systematic analyses alone have had limited success in resolving relationships between hyperiid lineages (e.g. Pirlot, 1932; Bowman and Gruner, 1973; Coleman, 1994; Vinogradov et al., 1996; Zeidler, 1999, 2003a, 2003b, 2004, 2006, 2009), independent molecular phylogenetic studies can be used to distinguish phylogenetically informative characteristics from convergently evolved traits (Browne et al., 2007). The identification of the former is necessary for inferring synapomorphic morphologies that define higher level relationships, whereas the latter are particularly useful for understanding the evolutionary origins of convergent morphologies. Specifically in the case of hyperiid amphipods, how biological form and function are linked to evolutionary radiations within oceanic midwater niches will inform the broader question of how patterns of biological diversity have arisen in the largest contiguous habitat on the planet.

Here we infer a molecular phylogenetic history of hyperiid amphipods in order to determine if morphological similarities among these pelagic forms have a common evolutionary history or represent convergent evolution. In order to sample a broad diversity of hyperiid amphipods, we used traditional net based collection techniques in combination with recent advances in submersible and SCUBA *in situ* midwater collection techniques. Multiple gene-tree and species-tree methods were used to analyze sequence data sets from the nuclear genes 18S rRNA, 28S rRNA, and *Histone H3* (*H3*) and the mitochondrial gene *cytochrome oxidase I* (*COI*). Results of gene-tree and species-tree analyses are compared and the utility of species-tree analyses for reconstructing ancient evolutionary histories is discussed. The resulting phylogenetic hypotheses are interpreted in the context of visual and olfactory modifications that may correspond with discrete midwater niches.

2. Materials and methods

2.1. Specimen collection

Hyperiid amphipods were collected (Table 3) via snorkeling, blue-water diving (Hamner, 1975; Hamner et al., 1975; Haddock and Heine, 2005) on both open-circuit (OC), and closed-circuit rebreather (CCR) SCUBA (Ambient Pressure Diving Ltd., UK), remotely operated underwater vehicles (MBARI), ring nets, and opening-closing trawling nets (Childress et al., 1978). Oceanic midwaters sampled include the Northeast, Northwest, and Central Pacific. In the Atlantic, the western edge of the Gulf Stream, the Caribbean, and the Weddell Sea were sampled. Physical vouchers exist for specimens and are housed at the University of Miami (Coral Gables, FL) and the Smithsonian NMNH (Washington, DC) (Table 3). Specimens of hyperiid amphipods were identified using the taxonomic keys of Bowman and Gruner (1973), Vinogradov et al. (1996), and Zeidler (1999, 2003a, 2003b, 2004, 2009). Two hyperiid taxa included in this analysis were not identified to species level. They have been assigned temporary names indicating their affinity to described species. Two isopod genera, *Cyathura* sp. and *Idotea* sp., were collected and sequences were used for outgroup comparison.

2.2. Sequence cloning

Genomic DNA was extracted using the DNeasy Tissue Kit (Qiagen, Inc.) from isolated pleopod and/or dissected and isolated trunk muscle tissue. Amplification of *Cytochrome Oxidase I* (*COI*), *Histone* (*H3*), 18S, and 28S ribosomal genes were completed using primers indicated in Table 1. PCR products of the appropriate size were direct sequenced by Macrogen, Inc (South Korea). All sequences have been deposited with GenBank (Table 3).

2.3. Phylogenetic analysis

2.3.1. Alignments

Sequences were aligned in ClustalX using default parameters. COI and H3 sequences were translated into protein sequences prior to alignment. Some regions of the ribosomal sequences (18S and 28S) were too divergent to be confidently aligned, therefore, the software program Gblocks v. 0.91b (Castresana, 2000) was used to identify poorly aligned regions for removal prior to further analysis. Gblock parameters were defined as follows: minimum number of sequences for a conserved position (50%), minimum number of sequences for a flanking position (50%), maximum number of contiguous non-conserved positions (10), minimum length of a block (5), and allowed gap positions (with half). Alignments after removal of non-conserved positions were 1465 bp and 2214 bp long for 18S and 28S, respectively.

2.3.2. Gene tree reconstructions

Evolutionary models for phylogenetic analyses were selected independently for each locus using MrModeltest (Nylander, 2004) under the Akaike Information Criterion (AIC). Phylogenetic reconstructions of concatenated and individual gene-trees were performed using both Bayesian Markov Chain Monte Carlo (MCMC) and Maximum Likelihood (ML) criteria. Bayesian reconstructions were performed using MrBayes 3.1.2 (Huelsenbeck and Ronquist, 2001; Ronquist and Huelsenbeck, 2003). For the MCMC analysis of concatenated datasets, each locus was assigned as a separate partition and rates were allowed to vary across partitions. Protein coding datasets (COI and H3) were further partitioned by codon site for a total of nine partitions. Bayesian analysis of concatenated datasets included two runs for 1×10^7 generations and analyses of datasets from individual loci were run for 1×10^6 generations (S1). Trees were sampled every 1000 generations using four Markov chains and default heating values and a burn-in fraction of 10%. Convergence was assessed by standard deviation of split-frequencies (<0.01) and by examining trace plots of log-likelihood scores in Tracer 1.5 (Rambaut and Drummond, 2007).

ML gene-trees were estimated using the software RAxML 7.0.3 (Stamatakis, 2006). For the concatenated dataset we employed the GTR + Γ model of evolution. The RAxML software accommodates the GTR model of nucleotide substitution with the additional options of modeling rate heterogeneity (Γ) and proportion invariable sites (I). Modeling of invariable sites is discouraged by the author as invariable sites are already accounted for when rate heterogeneity is included in the model; including both parameters may be problematic as they cannot be estimated independently. The concatenated dataset was partitioned by loci and protein coding sequences were further partitioned by codon site; substitution rates and α-shape parameters were optimized separately for each partition. Three separate ML searches were run from different randomized maximum parsimony trees. Nonparametric bootstrapping (100 replicates) was used to estimate support values at each node. These analyses utilized the rapid bootstrapping algorithm (i.e. option –f a in RAxML). Bootstrapped trees were pooled across runs and the ML tree is displayed with pooled bootstrap values shown at the nodes (S2).

2.3.3. Species-tree reconstructions

To reconstruct species-trees from our four locus dataset we used the parsimony-based Minimize Deep Coalescence (MDC) method. MDC analyses were performed using the software

Table 1
List of PCR primers used.

Gene	Primer	Sequence (5′–3′)	Reference
COI	LCO1490	GGTCAACAAATCATAAAGATATTGG	Folmer et al. (1994)
	HCOoutout	GTAAATATATGRTGDGCTC	Schwendinger and Giribet (2005)
H3	H3aF	ATGGCTCGTACCAAGCAGACVGC	Colgan et al. (1998)
	H3aR	ATATCCTTRGGCATRATRGTGAC	Colgan et al. (1998)
18S	18S1F	TACCTGGTTGATCCTGCCAGTAG	Giribet et al. (1996)
	18S3F	GTTCGATTCCGGAGAGGGA	Giribet et al. (1996)
	18S4F	CCAGCAGCCGCGCTAATTC	Giribet et al. (1996)
	18S5F	GCGAAAGCATTTGCCAAGAA	Giribet et al. (1996)
	18S7F	GCAATAACAGGTCTGTGATGCCC	Giribet et al. (1996)
	18S7R	GCATCACAGACCTGTTATTGC	Giribet et al. (1996)
	18S5R	CTTGGCAAATGCTTTCGC	Giribet et al. (1996)
	18Sbi	GAGTCTCGTTCGTTATCGGA	Whiting et al. (1997)
	18S9R	GATCCTTCCGCAGGTTCACCTAC	Giribet et al. (1996)
28S	28Srd1a	CCCSCGTAAYTTAGGCATAT	Mallatt and Sullivan (1998)
	28Sa	GACCCGTCTTGAAACACGGA	Whiting et al. (1997)
	28Srd4.8a	ACCTATTCTCAAACTTTAAATGG	Mallatt and Sullivan (1998)
	28Sb	TCGGAAGGAACCAGCTAC	Whiting et al. (1997)
	28Srd5b	CCACAGCGCCAGTTCTGCTTAC	Mallatt and Sullivan (1998)
	28Srd7b1	GACTTCCCTTACCTACAT	Mallatt and Sullivan (1998)

program Phylonet (Than and Nakhleh, 2009) (i.e. option –m MDC). The MDC tree-search algorithm used by Phylonet differs from other heuristic search methods (Maddison and Maddison, 2010); Phylonet uses integer linear programming to find the exact species-tree topology that minimizes the number of conflicts (deep-coalescent events) among independent gene-trees (Maddison, 1997; Maddison and Knowles, 2006). MDC trees were evaluated using both majority-consensus Bayesian gene-trees and ML gene-trees as input topologies (evolutionary models and run parameters described above). All input gene-trees were rooted using *Cyathura* sp. and *Idotea* sp. as outgroups.

3. Results

3.1. Genetic variation

Sequence products were obtained for all four loci from all 51 of the sampled taxa. PCR products for the four loci averaged 810 bp, 360 bp, 1570 bp and 2790 bp for COI, H3, 18S and 28S, respectively (Table 2). Clustal alignments of the COI dataset resulted in 8 indels ranging in length from three to nine basepairs. Alignments were performed on translated datasets for COI and H3 and no frameshift indels occurred in the final alignment. No indels occurred in the final alignment of the H3 dataset. Alignment of datasets for both the 18S and 28S ribosomal genes resulted in a large number of indels ranging in length from 1 to 82 bp for the 18S alignment and 1 to 106 bp for the 28S alignment. Length of aligned datasets, variable and parsimony informative sites, and best fitting model are summarized in Table 2.

3.2. Phylogenetic analyses

3.2.1. Concatenated dataset

Gene trees recovered from ML and Bayesian analysis of concatenated datasets have nearly identical topologies (Bayesian tree with corresponding ML bootstrap support values is shown in Fig. 1). Both the ML and Bayesian analyses recovered four major clades with 100% posterior probability/bootstrap support: Physosomata, Phrominoidea, Platysceloidea, and Vibilioidea. Physosomata is traditionally recognized as its own infraorder (Bowman and Gruner, 1973). Our analyses discovered robust support for the inclusion of two enigmatic monogeneric families, the Cystisomatidae and Paraphronimidae, as branching basally to this group. Within Physosomata, we also recovered the two principal superfamilies supported by previous morphological investigation, the Scinoidea and Lanceoloidea. Among the Scinoidea our concatenated gene analysis supports a sister group relationship between *Acanthoscina* and *Mimonectes* with *Scina* branching basally. For the Lanceoloidea our concatenated gene analysis discovered strong support for the neotonic *Microphasma*, a member of the Microphasmidae, as branching from within the *Lanceola*, a member of the Lanceolidae. Finally, we discovered *Scypholanceola* to be robustly supported as having more than one branch within the *Lanceola*. Thus we infer that the Lanceoloidea, as currently recognized, is polyphyletic.

The three remaining clades, Phrominoidea, Platysceloidea, and Vibilioidea, are reciprocally monophyletic and broadly contain taxa from the traditionally defined infraorder Physocephalata (Bowman and Gruner, 1973). The basal-most branching clade is comprised of the Phronimoidea. Our analysis inferred strong support for a sister group relationship between the Phronimidae (*Phronima* + *Phronimella* in this study) and the Phrosinidae (*Phrosina* + *Primno* in this study). Our results also strongly support a clade composed of *Hyperioides*, *Hyperietta*, and *Lestrigonus* as the Lestrigonidae proposed by Zeidler (2004). The Lestrigonidae have robust support for sister group relationship with the Hyperiidae *sensu* Zeidler (2004). Within the Hyperiidae we discovered strong support for the group that includes the genera *Iulopis*, *Hyperoche*, *Hyperia*, and *Themisto*. Among the Hyperiidae the principal difference between our concatenated Bayesian and ML results is the position of the genus *Themisto*. In

Table 2
Polymorphism data summary and best fitting model for all loci.

Locus	Length of PCR products (bp)	Best fitting model (P. inv)	Empirical base frequencies G/A/T/C	Variable sites	Parsimony informative sites
COI	749–839	GTR + I + Γ (0.23)	0.13/0.34/0.41/0.12	615/852	548/852
H3	328	GTR + I + Γ (0.55)	0.24/0.24/0.25/0.24	136/328	124/328
18S	1520–2270	GTR + Γ	0.29/0.22/0.23/0.26	857/1465	754/1465
28S	1283–3162	GTR + Γ	0.28/0.21/0.25/0.26	2203/2203	2199/2203

Table 3
Alphabetical listing of hyperiid species used in this study including collection locality, voucher information, and GenBank accession numbers.

Taxon	Collection			Physical vouchers		Genbank accession			
	Locality	Latitude	Longitude	USNM	gDNA	*COI*	*H3*	18S	28S
Acanthoscina acanthodes	Fort Pierce, FL, USA	27.34°N	79.54°W	1196364	AP055	EF989700	KC428931	KC428880	KC428829
Brachyscelus crusculum	Kona coast, HI, USA	19.42°N	156.07°W	1196359	AP049	EF989658	KC428932	KC428881	KC428830
Brachyscelus globiceps	Kona coast, HI, USA	19.35°N	156.00°W	1196358	AP046	EF989660	KC428933	KC428882	KC428831
Brachyscelus rapax	Green Bay, PAN	9.14°N	82.14°W	1196351	AP026	EF989659	KC428934	KC428883	KC428832
Calamorhynchus pellucidus	Oahu, HI, USA	21.12°N	158.19°W	1196372	AP065	EF989649	KC428935	KC428884	KC428833
Cranocephalus scleroticus	Kona coast, HI, USA	19.35°N	156.00°W	n/a	AP041	EF989648	KC428936	KC428885	KC428834
Cyathura sp.	Woods Hole, MA, USA	41.31°N	70.40°W	n/a	n/a	AF520451	KC428937	KC428886	KC428835
Cyllopus lucasii	Weddell Sea	60.94°S	53.12°W	n/a	AP070	EF989691	KC428938	KC428887	KC428836
Cyllopus magellanicus	Weddell Sea	60.94°S	53.12°W	1196376	AP069	EF989690	KC428939	KC428888	KC428837
Cystisoma gershwinae	California, USA	36.58°N	122.50°W	n/a	AP018	EF989675	KC428940	KC428889	KC428838
Cystisoma pellucida	California, USA	36.43°N	124.07°W	1196343	AP003	EF989676	KC428941	KC428890	KC428839
Glossocephalus milneedwardsi	Pelican Cayes, BZ	16.40°N	88.11°W	1196342	AP002	EF989654	KC428942	KC428891	KC428840
Glossocephalus sp.	California, USA	36.60°N	122.37°W	n/a	AP019	EF989655	KC428974	KC428923	KC428872
Hyperia macrocephala	Weddell Sea	60.56°S	52.81°W	1196375	AP068	EF989666	KC428943	KC428892	KC428841
Hyperietta parviceps	Kona coast, HI, USA	19.35°N	156.00°W	1196357	AP045	EF989686	KC428944	KC428893	KC428842
Hyperioides longipes	Fort Pierce, FL, USA	27.34°N	79.54°W	1196360	AP050	EF989685	KC428945	KC428894	KC428843
Hyperoche capucinus	Weddell Sea	60.56°S	52.81°W	1196380	AP079	EF989665	KC428946	KC428895	KC428844
Hyperoche martinezi	California, USA	36.37°N	122.10°W	1196346	AP006	EF989668	KC428947	KC428896	KC428845
Hyperoche medusarum	California, USA	35.80°N	122.85°W	1196348	AP009	EF989667	KC428948	KC428897	KC428846
Idotea sp.	Woods Hole, MA, USA	41.31°N	70.40°W	n/a	n/a	KC428828	KC428949	KC428898	KC428847
Iulopis loveni	Fort Pierce, FL, USA	27.34°N	79.54°W	1196361	AP052	EF989669	KC428950	KC428899	KC428848
Lanceola loveni	California, USA	36.37°N	122.09°W	n/a	AP033	EF989693	KC428951	KC428900	KC428849
Lanceola pacifica	California, USA	35.50°N	123.87°W	n/a	AP021	EF989697	KC428952	KC428901	KC428850
Lanceola sayana	California, USA	36.43°N	124.07°W	n/a	AP035	EF989696	KC428953	KC428902	KC428851
Leptocotis tenuirostris	Fort Pierce, FL, USA	27.34°N	79.54°W	1196355	AP042	EF989653	KC428954	KC428903	KC428852
Lestrigonus schizogeneios	Kona coast, HI, USA	19.35°N	156.00°W	1196352	AP030	EF989684	KC428955	KC428904	KC428853
Lycaea nasuta	Kona coast, HI, USA	19.42°N	156.07°W	1196356	AP044	EF989647	KC428956	KC428905	KC428854
Microphasma agassizi	California, USA	36.43°N	124.07°W	1196381	AP080	EF989692	KC428957	KC428906	KC428855
Mimonectes loveni	California, USA	36.60°N	122.38°W	1196365	AP056	EF989698	KC428958	KC428907	KC428856
Oxycephalus clausi	Oahu, HI, USA	21.29°N	158.23°W	1196371	AP063	EF989652	KC428959	KC428908	KC428857
Paraphronima gracilis	California, USA	36.43°N	124.07°W	1196368	AP059	EF989674	KC428960	KC428909	KC428858
Parapronoe cambelli	Oahu, HI, USA	21.12°N	158.19°W	1196373	AP066	EF989657	KC428961	KC428910	KC428859
Phronima bucephala	California, USA	36.43°N	124.07°W	1196349	AP011	EF989680	KC428962	KC428911	KC428860
Phronimella elongata ATL	Fort Pierce, FL, USA	27.34°N	79.54°W	n/a	AP014	EF989677	KC428963	KC428912	KC428861
Phronimella elongata PAC	Oahu, HI, USA	21.26°N	158.20°W	1196366	AP057	EF989678	KC428964	KC428913	KC428862
Phrosina semilunata ATL	Fort Pierce, FL, USA	27.34°N	79.54°W	1196353	AP037	EF989670	KC428965	KC428914	KC428863
Phrosina semilunata PAC	Oahu, HI, USA	21.27°N	158.14°W	1196367	AP058	EF989671	KC428966	KC428915	KC428864
Primno brevidens	California, USA	36.37°N	122.10°W	1196345	AP005	EF989672	KC428967	KC428916	KC428865
Primno evansi	Fort Pierce, FL, USA	27.34°N	79.54°W	1196354	AP038	EF989673	KC428968	KC428917	KC428866
Rhabdosoma whitei	Oahu, HI, USA	21.13°N	158.16°W	1196369	AP061	EF989650	KC428969	KC428918	KC428867
Scina borealis	California, USA	36.33°N	122.90°W	1196363	AP054	EF989699	KC428970	KC428919	KC428868
Scypholanceola aestiva	California, USA	36.43°N	124.07°W	n/a	AP034	EF989694	KC428972	KC428921	KC428870
Scypholanceola sp.	California, USA	35.48°N	123.86°W	1196344	AP004	EF989695	KC428971	KC428920	KC428869
Streetsia challengeri	Oahu, HI, USA	21.27°N	158.14°W	1196370	AP062	EF989651	KC428973	KC428922	KC428871
Themsito japonica	Hokkaido, JN	42.00°N	141.00°E	1196378	AP076	EF989663	KC428975	KC428924	KC428873
Themsito pacifica	California, USA	36.43°N	124.07°W	1196362	AP053	EF989664	KC428976	KC428925	KC428874
Thyropus sphaeroma	Oahu, HI, USA	21.12°N	158.19°W	1196374	AP067	EF989661	KC428977	KC428926	KC428875
Tryphana malmi	California, USA	36.80°N	121.80°W	1196379	AP078	EF989656	KC428978	KC428927	KC428876
Vibilia antartica	Weddell Sea	60.94°S	53.12°W	1196377	AP073	EF989689	KC428979	KC428928	KC428877
Vibilia propinqua	California, USA	35.46°N	122.50°W	1196347	AP007	EF989687	KC428980	KC428929	KC428878
Vibilia viatrix	California, USA	35.30°N	123.52°W	1196350	AP020	EF989688	KC428981	KC428930	KC428879

the Bayesian analysis *Iulopis* branches at the base of the Hyperiidae and *Themisto* is highly supported as branching from within the *Hyperoche* which lends additional support to *Hyperoche* currently representing a polyphyletic assemblage. However in our ML tree *Themisto* branches at the base of Hyperiidae.

Among the clade composed of the Platysceloidea our analysis strongly supported the sister grouping of *Tryphana* (Tryphanidae) with *Thyropus* (Parascelidae) at the base of the Platysceloidea. The Brachyscelidae are highly supported as sister to the Oxycephalidae. Within the Oxycephalidae (*Rhabdosoma, Lycaea, Glossocephalus, Leptocotis, Streetsia, Cranocephalus, Calamorhynchus* and *Oxycephalus* in this study) *Rhabdosoma* is highly supported as branching basally. While we discovered high support for the monophyly of the Oxycephalidae, the ML bootstrap values were generally low for many internal branching nodes. The Vibilioidea clade is composed of two well supported, reciprocally monophyletic groups, the Vibiliidae and the monogeneric Cyllopodidae.

3.2.2. Individual gene trees

Both Bayesian and ML gene trees supported the four major clades identified in the concatenated gene-tree for three out of four loci (COI, 18S and 28S; Fig. 1). The Histone H3 gene-tree was poorly resolved in both Bayesian and ML reconstructions. Bayesian and ML trees for individual loci are depicted in the Supplementary material (S1 and S2, respectively). Species that were represented by more than one specimen remained monophyletic for all analyses. Relationships among major clades and several basal taxa did vary among the gene-trees we analyzed. Specifically, the placement of the Vibilioidea differs between the COI tree and the nuclear gene trees (S1, S2). Also there are two taxa, *Tryphana malmi* and *Paraphronima gracilis*, that fall outside the three/four major clades

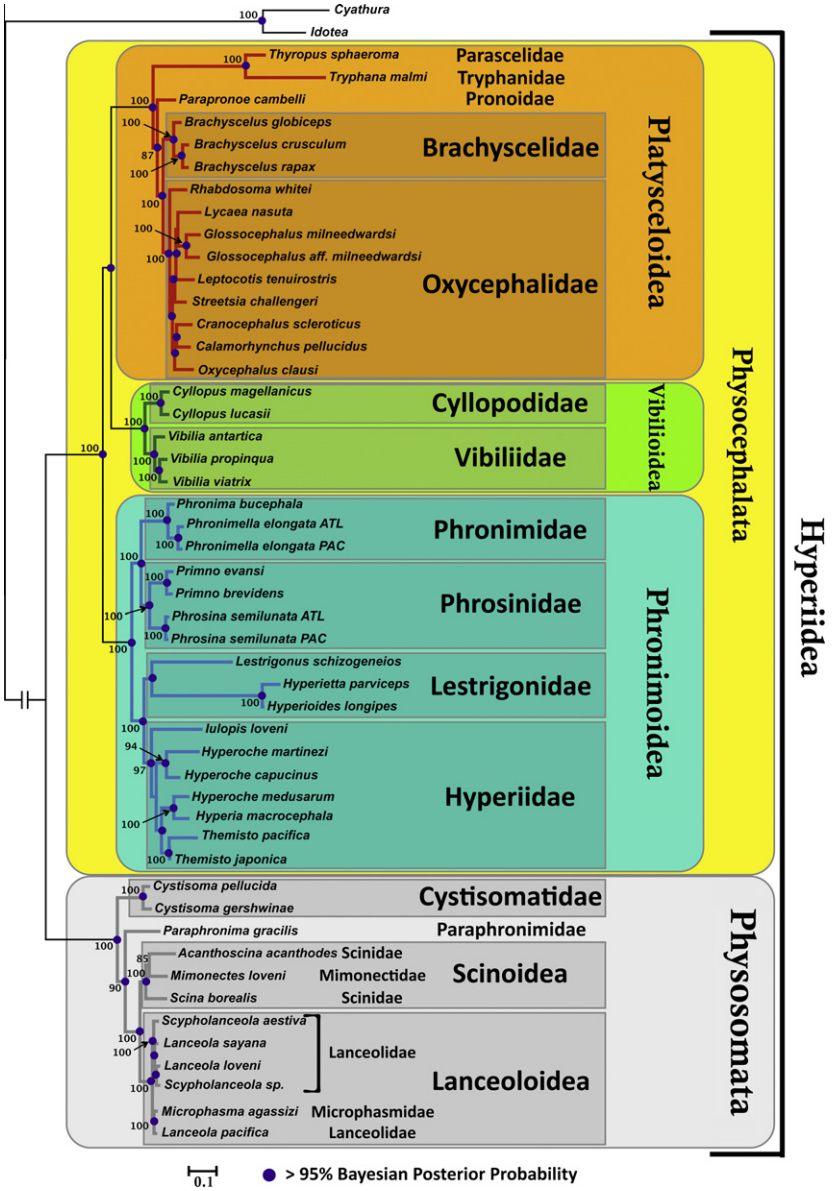

Fig. 1. Combined species-tree estimates for the concatenated dataset using Bayesian criterion as performed by MrBayes and maximum-likelihood (ML) criterion as performed by RaxML. Node labels indicate posterior probability support >95% and boostrap support >85% for Bayesian and ML trees, respectively.

and whose placement varied greatly among the individually analyzed loci. Given the observations of gene tree heterogeneity across nuclear loci a species tree approach to the phylogenetic reconstruction of hyperiid relationships was warranted (Knowles and Kubatko, 2010).

3.2.3. MDC Species tree results

Results from our MDC analyses based on both Bayesian and ML input trees recovered the same four major clades observed in the concatenated gene trees (Fig. 2). However the two MDC topologies disagreed on the relationships between the three clades comprising the infraorder Physocephalata. MDC analysis based on Bayesian input trees placed the Vibilioidea as sister group to the Platysceloidea consistent with the results obtained from both concatenated tree analyses (Fig. 2a). Whereas MDC analysis of ML input trees grouped the Vibilioidea with the Phronimoidea (Fig. 2b). Between the two different MDC analytical methods rearrangements among terminal taxa within the Oxycephalidae was observed. Within the infraorder Physosomata neither MDC analysis recovered a monophyletic Scinoidea. Additionally, rearrangements among terminal taxa within the Lanceoloidea were also observed.

4. Discussion

4.1. Significance to pelagic midwater hyperiid amphipod phylogeny

Our analysis discovered significant support for the placement of several problematic groups that have been historically difficult to reconcile based on morphology alone. For example the relationship of both *Cystisoma* and *Paraphronima* to other hyperiids based on morphological evidence has been unclear (Vinogradov et al., 1996; Zeidler, 2003a, 2003b). Classically these two genera have been unsatisfactorily placed in the Vibilioidea, based solely upon the morphology and position of the first antennae (Bowman and Gruner, 1973). In addition, both *Cystisoma* and *Paraphronima* independently possess suites of synapomorphies that have made classical taxonomic treatment perplexing. For example attempts to remove *Cystisoma* from the Vibilioidea based on unique

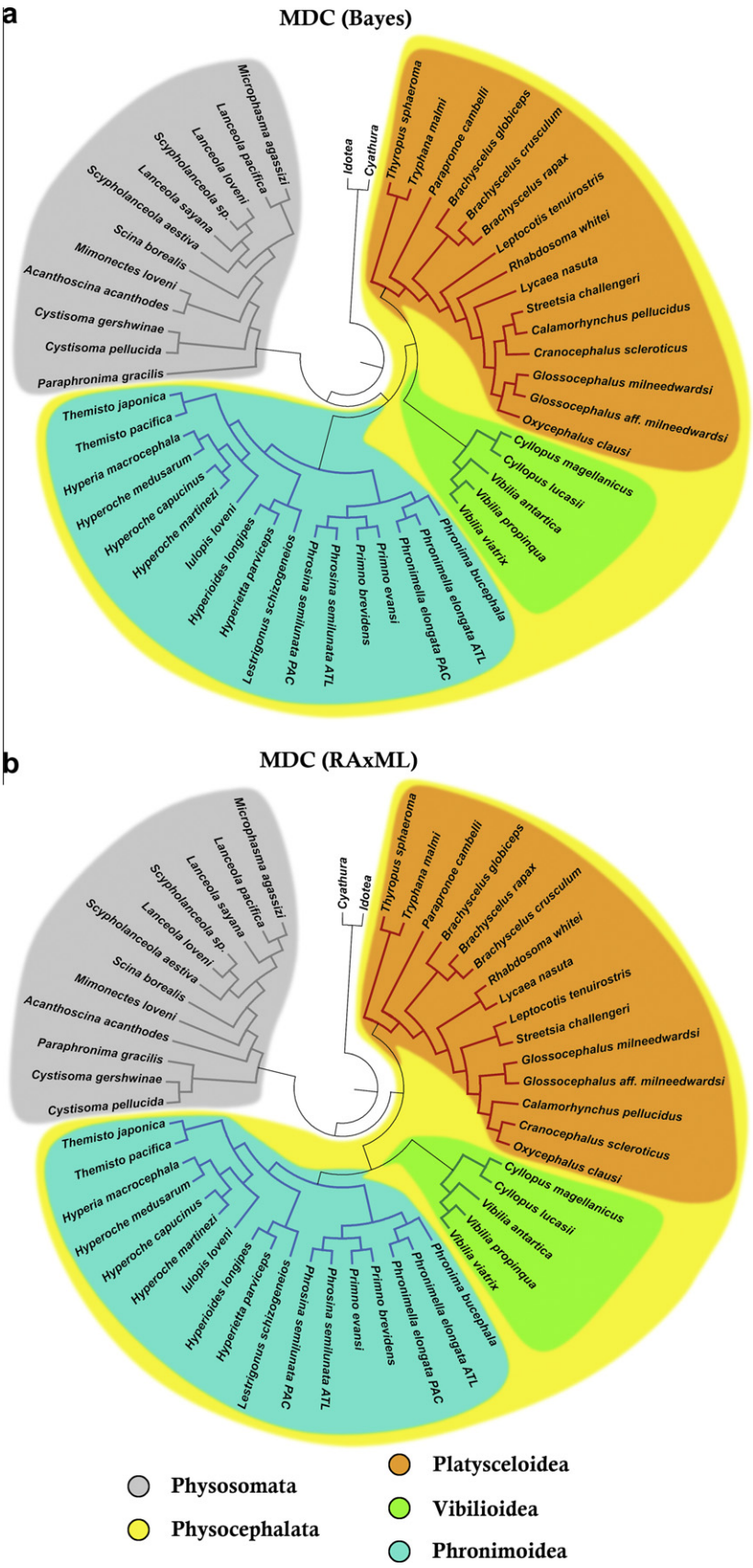

Fig. 2. Species-tree estimates based on Minimize Deep Coalescent (MDC) criterion as performed by Phylonet. Input tree topologies were generated using (a) Bayesian and (b) ML criterion (deep coalescent events for MDC trees numbered 114 and 69 for Bayesian and ML analyses, respectively). Individual gene trees are shown as Supplemental data (S1 and S2).

attributes of the head and reproductive structures has resulted in an unwieldy artificial arrangement of a superfamily, Cystisomatoidea, composed of a single monogeneric family, the Cystisomatidae, with a single genus, *Cystisoma* (Zeidler, 2003a). *Cystisoma* is often found at the limit of down welling sunlight and the hypertrophied eye field is completely dorsalyzed (Fig. 3a and b). The anterior brain has also been significantly modified in *Cystisoma* with nerve fibers innervating a highly dispersed retina (Land, 1981; Fig. 3c). In contrast to all other amphipods, *Cystisoma* embryos are retained in an internalized brood chamber (Brusca, 1981; Fig. 3a–c).

Both concatenated gene tree and species tree analyses advocate a natural classification in which *Cystisoma* is highly supported as the basal most branch of the Physosomata (Figs. 1 and 2); this placement is consistent with earlier analysis of *COI* data (Browne et al., 2007; supplemental data). The Physosomata have classically been defined as inhabiting deep bathypelagic and abyssopelagic midwater depths, possessing a 'swollen/inflated' pereon, a 'short' head, small or absent eyes, a proximally enlarged first antennae, mandibles without a molar process, and a first maxilla possessing an inner lobe (reviewed in Vinogradov et al., 1996). In support of the placement advocated here, *Cystisoma* has been described as possessing an inflated pereon (Vinogradov et al., 1996), genital papillae (Zeidler, 2006), as well as possessing a juvenile form originally described as physosoma by Wolterek (1903). The presence of classical Physosomata features in the juveniles of *Cystisoma*, such as a spherical pereon and small head, also lend support to the idea that the Physosomata are broadly composed of taxa retaining neotonic features.

Our analyses also strongly promotes the reassignment of the monogeneric family Paraphronimidae, containing *Paraphronima*, to the Physosomata. The multi-locus result generated strong support for *Paraphronima* branching between *Cystisoma* and the remainder of the Physosomata (Fig. 1). MDC Bayes inference places *Paraphronima* basal most within the Physosomata (Fig. 2a). MDC RAxML inference groups *Paraphronima* with *Cystisoma* (Fig. 2b). In contrast to the majority of the members of Physosomata both *Cystisoma* and *Paraphronima* inhabit dimly sunlit mesopelagic depths, participate in diel migrations, and possess very large heads with spectacularly hypertrophied eyes (Fig. 3a–f). Our analyses find the traditionally defined infraorder Physosomata to be paraphyletic and it should be redefined to include both Cystisomatidae and Paraphronimidae. The phylogenetic scenarios presented here suggest the superfamily distinction Cystisomatoidea for Cystisomatidea is invalid.

Within the Scinoidea both *Acanthoscina* and *Scina* have traditionally been included in the family Scinidae whereas *Mimonectes* is considered a member of the family Mimonectidae defined by the possession of several neotonic features. In contrast to the arrangement proposed by Vinogradov et al., 1996 in which the Mimonectidae branch basal to the Scinidae, we discovered support for *Mimonectes* branching between *Scina* and *Acanthoscina* (Fig. 1) suggesting that the Scinidae as currently defined may be polyphyletic. Both MDC analyses also recover a polyphyletic Scinidae with high support. Additional sampling within the Scinoidea is necessary to evaluate the validity of currently recognized family level relationships with the group. Phylogenetic placement of members of the Proscinidae would be particularly useful in this regard.

Within the Lanceoloidea we discovered strong support across our analyses for the neotonic *Microphasma*, a member of the Microphasmidae, as branching from within the *Lanceola*, a member of the Lanceolidae (Figs. 1 and 2). We also infer robust support for *Scypholanceola*, a genus within the Lanceolidae defined primarily by atypical cuticular morphology associated with their reduced eyes (Fig. 3g and h), to have more than one branch within the *Lanceola* (Figs. 1 and 2). Thus we suggest that the Lanceoloidea as currently recognized (Vinogradov et al., 1996) is polyphyletic. In this scenario the cuticular modifications associated with the eyes of *Scypholanceola* would be convergent adaptations and thus not useful as phylogenetically informative characters. Additional sampling among the Lanceolidae is certainly warranted given our results. Information from members of the Chuneolidae will also be useful in defining relationships within the Lanceoloidea.

Both multi-locus and MDC results recover the monophyletic infraorder Physocephalata. The Physocephalata have classically been defined as inhabiting sunlit epipelagic and mesopelagic water depths. In contrast to deep water taxa, the Physocephalata typically display varying degrees of transparency, possess large heads with well developed eyes, have mandibles with a molar process, a first maxilla possessing an inner lobe, and males generally have long antennal flagellum (reviewed in Vinogradov et al., 1996). Our molecular analyses recover three major clades within the Physocephalata previously identified by morphology alone; the Vibilioidea, the Platysceloidea, and the Phronimoidea. With respect to the Vibilioidea, our analyses broadly advocate removing both *Cystisoma* and *Paraphronima* and support redefining Vibilioidea to include the Vibiliidae (represented by *Vibilia* in this study) as reciprocally monophyletic to the Cyllopodidae (*Cyllopus*) *sensu* Zeidler (2003b). In contrast to most other Physocephalata the eyes of Vibiliidae are variable in size and do not encompass the entire head. *Cyllopus* (Cyllopodidae) however does retain the hypertrophied eye characteristics of most Physocephalata. While our multi-locus concatenated gene tree and MDC Bayes species tree consistently recovered the Vibilioididea as sister to Platysceloidea, the MDC RAxML result recovered Vibilioididea as sister to the Phronimoidea.

Members of the clade comprised by the Platysceloidea predominantly inhabit the well lit uppermost epipelagic region of the water column. Males in this group possess unique sexually dimorphic characters associated with both first and second pairs of antennae (reviewed in Vinogradov et al., 1996). Within the Platysceloidea the placement of the monotypic *Tryphana* based on morphology and *COI* has been problematic (Vinogradov et al., 1996; Browne et al., 2007). Our analysis inferred strong support across both the multi-locus concatenated tree and MDC analyses for a clade that includes *Thyropus* and *Tryphana* that branches basally within the Platysceloidea. Additional sampling within Parascelidea and Platyscelidae should be pursued to confirm this result. The position of the *Lycaea* within Platysceloidea based on morphology has also been difficult. Earlier analysis of *COI* placed *Lycaea* close to *Glossocephalus* in the Oxycephalidae but with poor support (Browne et al., 2007). Our results discovered additional strong support for the position of *Lycaea* within the Oxycephalidae. Thus we suggest that the family Lycaeidea may be invalid and Oxycephalidae should be redefined to include the genus *Lycaea*. Additional sampling of *Lycaea*, and importantly *Simorhynchotus*, should also be pursued to confirm this result.

Members of the clade comprised of the Phronimoidea are well represented at both epipelagic and mesopelagic depths. Males in this group possess unique sexually dimorphic characters associated with the first and second pairs of antennae (reviewed in Vinogradov et al., 1996). Within the Phronimoidea we discovered strong support for two reciprocally monophyletic groups the Phronimidae + Phrosinidae clade and the Lestrigonidae + Hyperiidae clade. Our analyses consistently recovered a monophyletic Lestrigodidae *sensu* Zeidler (2004), represented in this study by *Lestrigonus*, *Hyperietta*, and *Hyperioides*. Among the Hyperiidae we found that *Hyperia* branches from within *Hyperoche* suggesting that *Hyperoche* as currently recognized is polyphyletic. The Phronimidae are united by a suite of head and eye modifications as well as the unique use of Thaliacean tissue to craft transparent 'barrels'

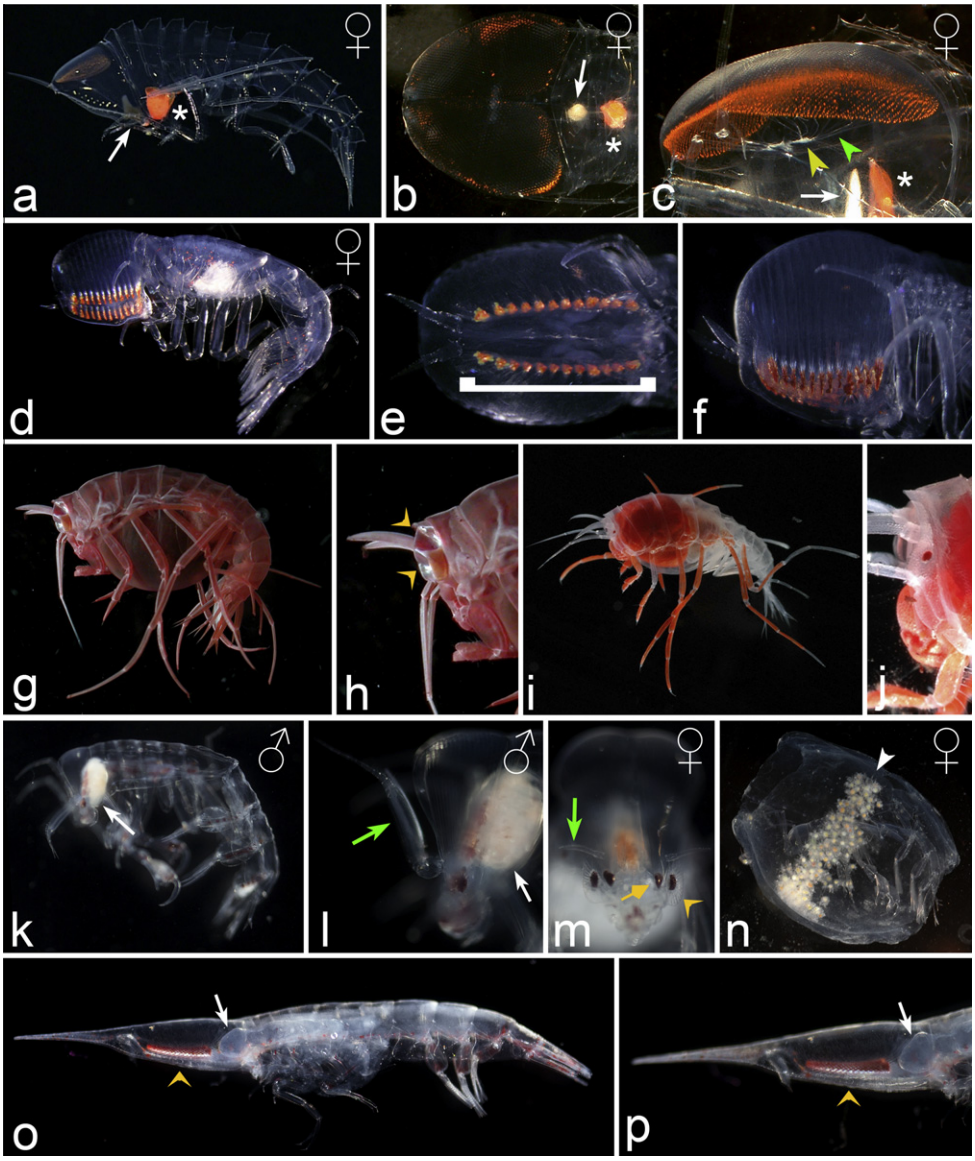

Fig. 3. Representative taxa from the two principal lineages of hyperiid amphipods. Unless otherwise noted, anterior is left and dorsal is towards top. (a) Lateral view of *Cystisoma pellucida*. *Cystisoma* possesses a single pair of hypertrophied eyes medially fused and directed dorsally. The white arrow marks the location of the foregut and stomach. The asterisk marks the location of the internalized brood chamber. (b) A dorsal view of the head and anterior pereon of *Cystisoma* highlighting the dispersed sheet-like organization of the retina. The white arrow marks the location of the foregut and stomach. The asterisk marks the location of the internalized brood chamber. (c) Anteriolateral view of *Cystisoma*. The extreme transparency of this species allows for identification of components of the nervous system in live animals. Here portions of the anterior protocerebrum (yellow arrowhead) and nerve tracts innervating the highly dispersed retina (green arrowhead) are indicated. (d) Lateral view of *Paraphronima gracilis*. The eyes of *Paraphronima* are extraordinarily hypertrophied dominating nearly the entire head capsule. (e) Ventral view of the head. The bracket demarcates the anterior to posterior array of twelve pairs of retina. (f) Lateral closeup of *Paraphronima* head highlighting location of pairs of retina arrayed from anterior to posterior in a ventralized cuticular groove with dorsally directed crystalline cones. (g) Lateral view of *Scypholanceola* sp. The intense red coloration is common in taxa inhibiting deep midwater niches. (h) Closeup of *Scypholanceola* head. The two orange arrowheads highlight the location of two pairs of cuticular cup-like depressions associated with their reduced eyes. (i) Lateral view of *Lanceola loveni*. (j) Closeup of *Lanceola* head. The greatly reduced eye field of *Lanceola loveni* is more typical of the deepwater Physosomata. (k) Lateral view of a male *Phronima sedentaria*. The white arrow marks the location of the foregut and stomach. (l) Closeup of *Phronima* head. The green arrow highlights the hypertrophied large setose sexually dimorphic first antennae of males. The white arrow marks the location of the foregut and stomach. (m) Anterioventral view of a female *Phronima sedentaria*. The green arrow highlights the greatly reduced first antennae of females. *Phronima* has two pairs of eyes, one pair is characterized by extremely elongated dorsally directed crystalline cones. The orange arrow marks the ventromedialy located retina of the dorsally directed eye. The other eye pair possesses short crystalline cones that are directed laterally and ventrally and are marked with an orange arrowhead. (n) A female *Phronima sedentaria* in a 'barrel' crafted from Thaliacean tissue. *Phronima* exhibit maternal brood care and the barrel serves as both a transport device as well as the first food source for juveniles. The white arrowhead indicates the position of a band of recently hatched *Phronima* feeding on the inner surface of the 'barrel'. The distribution of juveniles in a tight medial belt within a barrel is typical. (o) Lateral view of *Streetsia challengeri*. *Streetsia* and related Oxycephalids are characterized by rostral extension of the head and hypertrophied eyes that dominate the head capsule. The orange arrowhead marks the position of the anterior-posteriorly elongated retina. The white arrow marks the location of the foregut and stomach. (p) Closeup of *Streetsia* head. The orange arrowhead marks the position of the anterior–posteriorly elongated retina. The white arrow marks the location of the foregut and stomach. (For interpretation of the references to color in this figure legend, the reader is referred to the web version of this article.)

used for transport as well as maternal brood care (Ball, 1977; Laval, 1978; Land, 1981; Fig. 3k–n). Their sister group, the Phrosinidae, possess analogous hypertrophic modifications of the fifth pereopod particularly with respect to the distal most elements.

4.2. Species trees methods assessment

It is now widely understood that phylogenetic reconstructions based on concatenated gene sequences are insufficient for

reconstructing species-level relationships (Degnan and Rosenberg, 2009). Both Bayesian and ML analyses of concatenated datasets often produce highly supported, yet incorrect species-tree topologies (Huang and Knowles, 2009; Liu and Edwards, 2009). Differences between gene-trees and species-trees due to incomplete lineage sorting are exacerbated when internal branch lengths are short relative to ancestral effective population sizes; a situation which describes the speciation history of most marine invertebrates (Degnan and Rosenberg, 2009; Knowles and Kubatko, 2010). To address this problem, a number of species tree methods including parsimony, likelihood, and Bayesian approaches, have been developed. These methods are routinely applied to phylogenetic questions of recent radiations where the number of OTUs is relatively small (i.e. <20) (Cranston et al., 2009; Linnen and Farrell, 2008; Hollingsworth and Hulsey, 2010). However, species-tree methods are rarely applied to broader scale phylogenetic questions with a greater number of OTUs.

Here we used parsimony species-tree methods to analyze a moderate sized dataset consisting of four loci from 51 OTUs. Our MDC analyses supported the existence of the same four major clades identified in the concatenation tree (Fig. 2). Disagreements among trees produced under different phylogenetic methods did occur at basal nodes, indicating that relationships among the four major clades are still unresolved. Despite strong support of basal nodes in the concatenated tree, disagreements between the species tree methods indicate that the current dataset does not contain enough information to confidently reconstruct these older evolutionary events. Additional loci and inclusion of more taxa are needed to increase the resolution at these basal nodes. Also, increased sampling within species may improve tree based inference using coalescent-based analyses such as *BEAST (Drummond and Rambaut, 2007; Heled and Drummond, 2010) and BEST (Liu, 2008). The sampling strategy employed for the present study included, in most cases, only one representative from each OTU. The inclusion of multiple samples per species is recommended for coalescent analysis as within-species polymorphisms contain valuable information regarding ancestral population sizes.

4.3. Conclusions

In summary we have been able to infer with a high degree of support two monophyletic radiations among pelagic amphipods; the Physosomata, inhabiting primarily bathypelagic depths and the Physocephalata, inhabiting primarily epipelagic and mesopelagic depths. Importantly our results have suggested placement of previously enigmatic taxa as well as highlighting problematic existing groupings. The analyses presented here strongly support the inclusion of *Cystisoma* and *Paraphronima* as basally branching taxa within the Physosomata clade and thus support the emergence of the Physosomata from an ancestral pelagic amphipod stem lineage that inhabited shallower regions of the water column in which downwelling light regimes played a significant role. However the relationship of Physosomata to the other major clade, the Physocephalata, remains undetermined and thus the issue of hyperiidean monophyly is unresolved.

The deep water Physosomata are largely characterized by an overall reduction in the size of the head and eyes relative to the body (e.g. Fig. 3i and j). In the absence of downwelling sunlight members of this clade often exhibit significant cuticle pigmentation, a common cryptic coloration strategy among deep sea organisms (Johnsen, 2005; e.g. Fig. 3g–j). In contrast the radiation of the Physocephalata in shallower oceanic midwaters has been strongly influenced by downwelling light regimes resulting in many members of this clade exhibiting varying degrees of transparency, a common crypsis strategy in well-lit pelagic environments (Johnsen, 2001; e.g. Fig. 3k–p). Most Physocephalata taxa also have large heads and eyes relative to their body length (e.g. Fig. 3o).

Traditional morphological analyses of hyperiids have generally been more focused on characters useful for systematic classification schemes and less focused on characters useful for determining phylogenetic groups. In particular characters associated with feeding morphologies have been heavily used in existing hyperiid systematic treatments (Bowman and Gruner, 1973; Vinogradov et al., 1996). However recent studies suggest these morphologies are particularly plastic among amphipods (e.g. Havermans et al., 2010). Thus character states associated with the presence or absence of mandibular palps and the reduction of the maxillae and maxillipeds (e.g. Vinogradov et al., 1996) are evolutionarily labile and may not accurately reflect evolutionary histories (Browne and Patel, 2000). Structural simplifications associated with abdominal epimerons and reductions of the uropods are also problematic. In contrast, our results suggest that structural elaborations, for example sexually dimorphic morphological hypertrophies associated with the first and second antennae, correlate remarkably well with our multi-locus molecular phylogenetic analyses. In light of our results additional sampling of hyperiid taxa is warranted to assess the validity of the proposed phylogenic relationships for this important group of midwater organisms.

The issue of hyperiid monophyly and other outstanding questions regarding relationships among the major amphipod radiations should be addressed more broadly by employing a taxon sampling strategy that seeks to increase representation among the major gammaridean amphipod groups in combination with a scalable phylogenomic strategy (Hejnol et al., 2009). This will ensure a large number of loci are sampled across a wide swath of amphipod diversity and will ultimately prove useful for examining relationships across a group that has historically proved recalcitrant to morphological analyses.

The gammaridean amphipod *Parhayle hawaiensis* has emerged as a powerful model system for both developmental and genomics studies within the crustaceans and offers a significant opportunity to delve into the details of specific developmental programs relevant to morphological attributes that appear to be important to the pelagic life history of hyperiid amphipods (Browne et al., 2005; Kontarakis et al., 2011; Zeng et al., 2011; Blythe et al., 2012). Future work on improving both phylogenetic inference and modeling morphological development in amphipods will allow us to begin to circumscribe the connections between genotype and phenotype that have generated the remarkable morphological diversity we see in the largest contiguous habitat on the planet, the oceanic midwaters.

Acknowledgments

This work has been supported by NSF (DBI-03100269, IOS-0718975, OCE-1125396), the David and Lucile Packard Foundation, and startup funds from University of Miami College of Arts and Sciences. This work benefited substantially from access to the following Smithsonian Institution field stations: Fort Pierce (Florida) as SMSFP Contribution #898, Carrie Bowe Caye (Belize) as CCRE Contribution #932, and STRI-Bocas del Toro (Panama). This work also benefited substantially from access to the following vessels: the MBARI RV Western Flyer and the UNOLS fleet vessels R/V Kilo Moana, R/V Point Sur, and R/V Wecoma (W1109C). We thank the UH Diving Safety Program for providing OC and CCR SCUBA training and support. Specimens critical to this study were contributed by; Robert Humphreys, Karen Osborn, Rebecca Hoover, Wolfgang Zeidler, and the pilots of MBARI's ROV's. We also thank many for meaningful discussions, both Barbara Witlock and James Baker for providing critical comments that have significantly improved this communication, two anonymous reviewers for their

thoughtful comments, and most critically Mark Martindale for latitude at the inception.

Appendix A. Supplementary material

Supplementary data associated with this article can be found, in the online version, at http://dx.doi.org/10.1016/j.ympev.2012.12.021.

References

Ball, E.E., 1977. Fine structure of the compound eyes of the midwater amphipod *Phronima* in relation to behavior and habitat. Tissue Cell 9, 521–536.

Blythe, M.J., Malla, S., Everall, R., Shih, Y.-H., Lemay, V., Moreton, J., Wilson, R., Aboobaker, A.A., 2012. High through-put sequencing of the *Parhyale hawaiensis* mRNAs and microRNAs to aid comparative developmental studies. PLoS ONE 7, e33784.

Bowman, T.E., Gruner, H.-E., 1973. The families and genera of Hyperiidea (Crustacea: Amphipoda). Smithsonian Contrib. Zool. 146, 1–64.

Browne, W.E., Haddock, S.H.D., Martindale, M.Q., 2007. Phylogenetic analysis of lineage relationships among hyperiid amphipods as revealed by examination of the mitochondrial gene, *cytochrome oxidase I* (COI). Integr. Compar. Biol. 47, 815–830.

Browne, W.E., Patel, N.H., 2000. Molecular genetics of crustacean feeding appendage development and diversification. Sem. Cell Develop. Biol. 11, 427–435.

Browne, W.E., Price, A.L., Gerberding, M., Patel, N.H., 2005. Stages of embryonic development in the amphipod crustacean, *Parhyale hawaiensis*. Genesis 42, 124–149.

Brusca, G.J., 1981. On the anatomy of Cystisoma (Amphipoda: Hyperiidea). J. Crustac. Biol. 1, 358–375.

Castresana, J., 2000. Selection of conserved blocks from multiple alignments for their use in phylogenetic analysis. Mol. Biol. Evol. 17, 540–552.

Childress, J.J., Barnes, A.T., Quetin, L.B., Robison, B.H., 1978. Thermally protecting cod ends for the recovery of living deep-sea animals. Deep-Sea Res. 25, 419–422.

Coleman, C.O., 1994. Comparative anatomy of the alimentary canal of hyperiid amphipods. J. Crustac. Biol. 14, 346–370.

Colgan, D.J., McLauchlan, A., Wilson, G.D.F., Livingston, S.P., Edgecombe, G.D., Macaranas, J., Cassis, G., Gray, M.R., 1998. Histone H3 and U2 snRNA DNA sequences and arthropod molecular evolution. Aust. J. Zool. 46, 419–437.

Cranston, K.A., Hurvitz, B., Ware, D., Stein, L., Wing, R., 2009. Species trees from highly incongruent gene trees in rice. Syst. Biol. 58, 500–589.

Degnan, J.H., Rosenberg, N.A., 2009. Gene tree discordance, phylogenetic inference and the multispecies coalescent. Tree 24, 332–340.

Drummond, A.J., Rambaut, A., 2007. BEAST: Bayesian evolutionary analysis by sampling trees. BMC Evol. Biol. 7, 214.

Folmer, O., Black, M., Hoeh, W., Lutz, R., Vrijenhoek, R., 1994. DNA primers for amplification of mitochondrial cytochrome c oxidase subunit I from diverse metazoan invertebrates. Mol. Mar. Biol. Biotechnol. 3, 294–299.

Gasca, R., Suarez-Morales, E., Haddock, S.H.D., 2007. Symbiotic associations between crustaceans and gelatinous zooplankton in deep and surface waters off California. Mar. Biol. 151, 233–242.

Giribet, G., Carranza, S., Baguna, J., Riutort, M., Ribera, C., 1996. First molecular evidence for the existence of a Tardigrada + Arthropoda clade. Mol. Biol. Evol. 13, 76–84.

Haddock, S.H.D., Heine, J.N., 2005. Scientific Blue-Water Diving. California Sea Grant.

Hamner, W.M., 1975. Underwater observations of blue-water plankton: logistics, techniques, and safety procedures for divers at sea. Limnol. Oceanogr. 20, 1045–1051.

Hamner, W.M., Madin, L.P., Alldredge, A.L., Gilmer, R.W., Hamner, P.P., 1975. Underwater observations of gelatinous zooplankton: sampling problems, feeding biology, and behavior. Limnol. Oceanogr. 20, 907–917.

Harbison, G.R., Biggs, D.C., Madin, L.P., 1977. The associations of Amphipoda Hyperiidea with gelatinous zooplankton – II. Associations with Cnidaria, Ctenophora, and Radiolaria. Deep-Sea Res. 24, 465–488.

Hartke, T.R., Fiser, C., Hohagen, J., Kleber, S., Hartmann, R., Koenemann, S., 2011. Morphological and molecular analyses of closely related species in the stygobiontic genus *Niphargus* (Amphipoda). J. Crustac. Biol. 31, 701–709.

Havermans, C., Nagy, Z.T., Sonet, G., Broyer, C.D., Martin, P., 2010. Incongruence between molecular phylogeny and morphological classification in amphipod crustaceans: a case study of *Antarctic lysianassoids*. Mol. Phylogenet. Evol. 55, 202–209.

Hejnol, A., Obst, M., Stamatakis, A., Ott, M., Rouse, G.W., Edgecombe, G.D., Martinez, P., Baguna, J., Bailly, X., Jondelius, U., Wiens, M., Muller, W.E.G., Seaver, E., Wheeler, W.C., Martindale, M.Q., Giribet, G., Dunn, C.W., 2009. Assessing the root of bilaterian animals with scalable phylogenomic methods. Proc. R. Soc. B 276, 4261–4270.

Heled, J., Drummond, A.J., 2010. Bayesian inference of species trees from multilocus data. Mol. Biol. Evol. 27, 570–580.

Huang, H., Knowles, L.L., 2009. What is the danger of the anomaly zone for empirical phylogenetics? Syst. Biol. 58, 527–536.

Huelsenbeck, J.P., Ronquist, F., 2001. MRBAYES: Bayesian inference of phylogeny. Bioinformatics 17, 754–755.

Hollingsworth, P.R., Hulsey, C.D., 2010. Reconciling gene trees of eastern North American minnows. Mol. Phylogenet. Evol. 61, 149–156.

Knowles, L.L., Kubatko, L.S., 2010. Estimating species trees: an introduction to concepts and models. In: Knowles, L.L., Kubatko, L.S. (Eds.), Estimating Species Trees: Practical and Theoretical Aspects. Wiley-Blackwell, New Jersey, pp. 1–14.

Kontarakis, Z., Pavlopoulos, A., Kiupakis, A., Konstantinides, N., Douris, V., Averof, M., 2011. A versatile strategy for gene trapping and trap conversion in emerging model organisms. Development 138, 2625–2630.

Land, M.F., 1981. Optics of the eyes of *Phronima* and other deep-sea amphipods. J. Comp. Physiol. A 145, 209–226.

Laval, P., 1978. The barrel of the pelagic amphipod *Phronima sedentaria* (Forsk.) (Crustacea: Hyperiidea). J. Exp. Mar. Biol. Ecol. 33, 187–211.

Linnen, C., Farrell, B., 2008. Comparison of methods for species-tree inverence in the sawfly genus *Neodiprion* (Hymenoptera: Diprionidae). Syst. Biol. 57, 876–890.

Liu, L., 2008. BEST: Bayesian estimation of species trees under the coalescent model. Bioinformatics 24, 2542–2543.

Liu, L., Edwards, S.V., 2009. Phylogenetic analysis in the anomaly zone. Syst. Biol. 58, 452–460.

Johnsen, S., 2001. Hidden in plan sight: the ecology and physiology of organsimal transparency. Biol. Bull. 201, 301–318.

Johnsen, S., 2005. The red and the black: bioluminescence and the color of animals in the deep sea. Integr. Comp. Biol. 45, 234–246.

Maddison, W.P., 1997. Gene trees in species trees. Syst. Biol. 46, 523–536.

Maddison, W.P., Knowles, L.L., 2006. Inferring phylogeny despite incomplete lineage sorting. Syst. Biol. 55, 21–30.

Maddison, W.P., Maddison, D.R., 2010. Mesquite: A Modular System for Evolutionary Analysis. Version 2.73. <http://mesquiteproject.org>.

Madin, L.P., Harbison, G.R., 1977. The associations of Amphipoda Hyperiidea with gelatinous zooplankton – I. Associations with Salpidae. Deep-Sea Res. 24, 449–463.

Mallatt, J., Sullivan, J., 1998. 28S and 18S rDNA sequences support the monophyly of lampreys and hagfishes. Mol. Biol. Evol. 15, 1706–1718.

Martin, J.W., Davis, G.E., 2001. An Updated Classification of the Recent Crustacea. Natural History Museum of Los Angeles County, Los Angeles.

Mills, C.E., 1993. Natural mortality in NE pacific coastal hydromedusae: grazing predation, wound healing, and senescence. Bull. Mar. Sci. 53, 194–203.

Nylander, J.A.A., 2004. MrModeltest v2. Program Distributed by the Author. Evolutionary Biology Centre, Uppsala University.

Pirlot, J.M., 1932. Introduction à l'Étude des Amphipodes Hypérides. Ann. L'Inst. Océanogr. 12, 1–36.

Rambaut, A., Drummond, A.J., 2007. Tracer v1.5. <http://beast.bio.ed.ac.uk/Tracer>.

Ronquist, F., Huelsenbeck, J.P., 2003. MRBAYES 3: Bayesian phylogenetic inference under mixed models. Bioinformatics 19, 1572–1574.

Schwendinger, P.J., Giribet, G., 2005. The systematics of the south-east Asian genus *Fangensis* Rambla (Opiliones: Cyphophthalmi: Stylocellidae). Invertebr. Syst. 19, 297–323.

Stamatakis, A., 2006. RAxML-VI-HPC: maximum likelihood-based phylogenetic analyses with thousands of taxa and mixed models. Bioinformatics 22, 2688–2690.

Than, C., Nakhleh, L., 2009. Species tree inference by minimizing deep coalescences. PLoS Comput. Biol. 5, e1000501.

Vinogradov, M.E., Volkov, A.F., Semenova, T.N., 1996. Hyperiid Amphipods (Amphipoda, Hyperiidea) of the World Oceans. Smithsonian Institution Libraries, Washington, DC.

Whiting, M.F., Carpenter, J.C., Wheeler, Q.D., Wheeler, W.C., 1997. The Strepsiptera problem: phylogeny of the holometabolous insect orders inferred from 18S and 28S ribosomal DNA sequences and morphology. Syst. Biol. 46, 1–68.

Wolterek, R., 1903. Bemerkungen zu den Amphipoda Hyperiidea der Deutschen Tiefsee-Expedition. I. Thaumatopsidae. Zool. Anz. 26, 447–459.

Zeidler, W., 1999. Review of the hyperiidean amphipod genus *Oxycephalus* Milne-Edwards (Crustacea: Amphipoda: Hyperiidea: Oxycephalidae). Invertebr. Taxon. 13, 391–424.

Zeidler, W., 2003a. A review of the hyperiidean amphipod family Cystisomatidae Willemoes-Suhm, 1875 (Crustacea: Amphipoda: Hyperiidea). Zootaxa 141, 1–43.

Zeidler, W., 2003b. A review of the hyperiidean amphipod superfamily Vibilioidea Bowman and Gruner, 1973 (Crustacea: Amphipoda: Hyperiidea). Zootaxa 280, 1–104.

Zeidler, W., 2004. A review of the families and genera of the hyperiidean amphipod superfamily Phronimoidea Bowman & Gruner, 1973 (Crustacea: Amphipoda: Hyperiidea). Zootaxa 567, 1–66.

Zeidler, W., 2006. A review of the hyperiidean amphipod superfamily Archaeoscinoidea Vinogradov, Volkov and Semenova, 1982 (Crustacea: Amphipoda: Hyperiidea). Zootaxa 1125, 1–37.

Zeidler, W., 2009. A review of the hyperiidean amphipod superfamily Lanceoloidea Bowman and Gruner, 1973 (Crustacea: Amphipoda: Hyperiidea). Zootaxa 2000, 1–117.

Zeng, V., Villanueva, K.E., Ewen-Campen, B.S., Alwes, F., Browne, W.E., Extavour, C.G., 2011. *De novo* assembly and characterization of a maternal and developmental transcriptome for the emerging model crustacean *Parhyale hawaiensis*. BMC Genom. 12, 581.